Three-tunnel-capacitor model for single-electron tunneling in layered thin films

T. G. Miller and R. Reifenberger
Department of Physics, Purdue University, West Lafayette, Indiana 47907
(Received 10 December 1993)

Measurements of the tunnel current as a function of applied voltage on the layered high-T_c material $TlBa_2(Ca_{0.8}Y_{0.2})Cu_2O_7$ have been shown to exhibit single-electron tunneling behavior. It has been proposed that the ultrasmall capacitance required to explain the single-electron tunneling spectra obtained with a low-temperature scanning tunneling microscope arises naturally from the planar crystal structure of this high-T_c material. This hypothesis is further examined using a single-electron tunneling model that incorporates three tunnel capacitors, a condition that is required by atomic-force-microscope studies of the topography of the film's surface. An improved fit to the tunneling conductance is obtained, providing further evidence that a key to understanding Coulomb blockade in layered materials like $TlBa_2(Ca_{0.8}Y_{0.2})Cu_2O_7$ is the tunnel capacitors that form between multilayer CuO planes. This conclusion has important implications for the fabrication of nanoelectronic devices based on single-electron effects.

I. INTRODUCTION

In a recent paper, the observation of single-electron charging (Coulomb staircase) was reported in a $TlBa_2(Ca_{0.8}Y_{0.2})Cu_2O_7$ film at 9.8 K.[1] The microscopic origin of this behavior is of considerable interest and it was suggested in Ref. 1 that the single-electron effects were due to the ultrasmall capacitance *between* the Cu-O layers of isolated islands that form naturally on this planar high-T_c material. The spectra were analyzed using a simple calculation based on two tunnel capacitors in series to roughly estimate the tunnel-capacitor parameters required to explain the data. Reasonable values consistent with the known properties of $TlBa_2(Ca_{0.8}Y_{0.2})Cu_2O_7$ were obtained.

A limitation of this earlier work was the questionable assumption that only two tunnel capacitors were required to explain the data. Since tunneling through many multilayers may occur in an isolated island formed on this layered material, it is important to consider whether a more realistic model provides an improved fit to the existing data. In what follows, using atomic force data to characterize the topography of the film's surface, we show that tunneling in this system is occurring through isolated islands that are two multilayers high. This observation demands that a three-tunnel-capacitor model be considered to fully explain the data.

In this paper we discuss such a three-tunnel-capacitor model and use it to fit the single-electron tunneling data previously obtained with a scanning tunneling microscope (STM). By calculating the single-electron behavior of three tunnel capacitors in series, we find an overall improvement in the fit to the data. This result suggests that the layered nature of high-T_c films provides an ideal material for forming vertical stacks of one-dimensional (1D) tunnel-capacitor arrays. These arrays are of considerable interest because of their potential application for single-electron nanoelectronic devices.

II. EXPERIMENTAL CONSIDERATIONS

It is useful to summarize the relevant experimental conditions that led to the Coulomb staircase behavior reported in Ref. 1. For the sake of completeness, a brief summary is provided below.

The data were obtained from a 0.3 μm thick $TlBa_2(Ca_{0.8}Y_{0.2})Cu_2O_7$ film as described previously.[1] Typical deposition parameters and growth conditions have been reported elsewhere.[2] The yttrium dopant substitutes at the calcium site and was added to increase the T_c of the material as well as reducing Tl loss at high temperatures.[2] Films grown by this method are highly epitaxial with the c axis perpendicular to the substrate surface.

Spectroscopic data $[I(V)]$ was acquired from an STM constructed to operate at low temperatures.[3] The design is similar to those previously published.[4–6] STM tips were formed from cut PtIr wires (0.25 mm diam). A diode temperature sensor mounted near the sample was used to monitor the temperature. Low-temperature measurements were made inside a vacuum insert that had been pumped out prior to cooldown.

Initial $I(z)$ measurements were used to verify that high quality tunnel junctions had been established, characterized by a tunnel current that decreased by orders of magnitude over a few angstroms.[3] After vacuum tunneling was clearly established, spectroscopic studies were performed. $I(V)$ measurements were made in which the computer feedback was paused, and the tip bias was ramped over the desired voltage range while the tunneling current was digitized. After one sweep, the feedback was momentarily enabled and the tip-sample separation was checked and adjusted in the usual way. Total acquisition time for each sweep was 75 msec or less. The derivative of the final $I(V)$, also referred to as the conductance, was obtained numerically.

0163-1829/94/50(5)/3342(8)/$06.00 ©1994 The American Physical Society

III. SURFACE STRUCTURE DETERMINED BY AFM

For the film studied, topographic data was obtained at low temperatures but was of poor quality. Isolated, caplike mounds (islands) were observed in regions where spectroscopic data were taken. To better characterize the surface of this material, further topographic data were obtained on the same sample with a commercial Park Scientific atomic force microscope (AFM) at room temperature. A representative image taken from the AFM room-temperature study is presented in Fig. 1.

This image is viewed from directly above. No filtering was performed but the image is displayed with a shading algorithm which simulates lighting from directly overhead. This has the effect of delineating terrace step edges in black, most of which are between 2.5 and 3.0 nm high (approximately two unit cells). One can clearly see large amounts of terracing which terminate in disconnected and isolated irregular islands. STM scans taken at low temperatures were of similar nature but characterized by a streaked and noisy behavior. Analysis of this data shows a significant number of islands with double unit cell heights and areas ranging from 1 to 100 square nanometers. Figure 2 is a histogram plot from AFM data taken over a one-square-micron area. In this plot, the vertical axis represents the percentage of the data within a specified range denoted on the horizontal axis. This figure has four dotted lines each exactly two unit cells (2.6 nm) apart. These fiducial lines clearly coincide with peaks in the height distribution indicating that double unit cell sized features are predominant. These islands are not to be confused with the overall grain size, which extends laterally on the order of microns. A cross section across one of the islands is shown in Fig. 3.

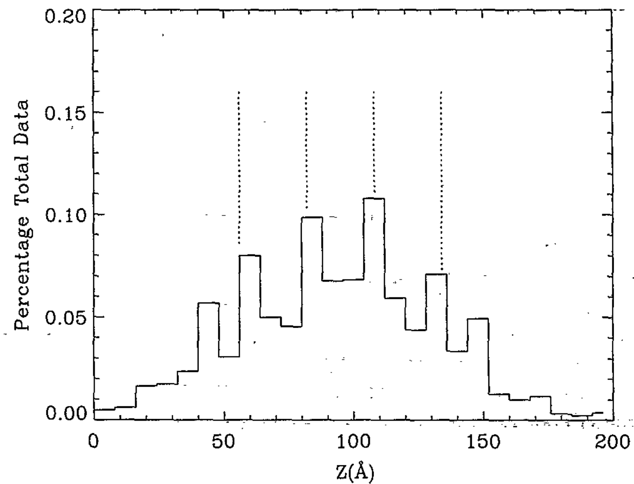

FIG. 2. A histogram analysis of data taken from a one-square-micron scan with an AFM at room temperature. The dotted lines are each spaced exactly two unit cells apart and illustrate the predominance of double unit cell islands in the data.

The representative topographical information shown in Fig. 3 provides a key insight into the detailed structure that must be included in a realistic model of the ultrasmall capacitance required to observe single-electron tunneling effects in these layered materials. Previous observations of single-electron effects on high-T_c materials have generally provided unsatisfactory explanations for the geometry necessary to produce the behavior observed. Typically a presumption is made that grains in the sample are somehow weakly coupled together in such a way as to produce the observed behavior. The difficulty with this explanation is that grain sizes in such materials are on the order of microns, producing capacitances far too large to explain the observed single-

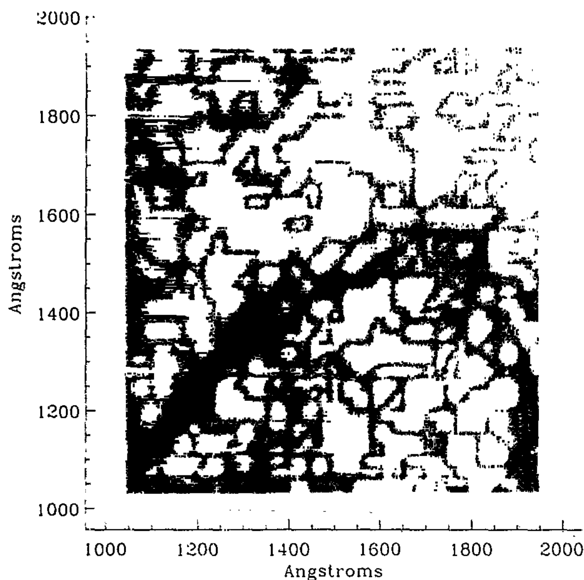

FIG. 1. Topographic data taken with an AFM on a $TlBa_2(Ca_{0.8}Y_{0.2})Cu_2O_7$ film at room temperature.

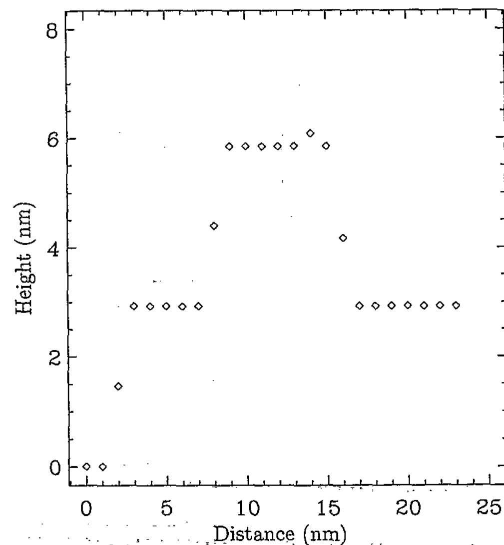

FIG. 3. A cross section taken from topographic AFM data on a $TlBa_2(Ca_{0.8}Y_{0.2})Cu_2O_7$ film at room temperature. This cross section shows a double unit cell high island resting on a terrace which is also two unit cells high.

electron effects. We believe a more likely explanation for the the ultrasmall capacitances lies in the layeredlike nature of the material itself.[1] Based on the room-temperature AFM scans, the origin of the single-electron tunneling can be naturally attributed to the isolated island structure found on the surface of this highly planar $TlBa_2(Ca_{0.8}Y_{0.2})Cu_2O_7$ material.

From the AFM topography, a realistic atomic-scale model for the tunneling geometry into an isolated island can be constructed as shown in Fig. 4. An important point to note is that when tunneling into such an island, the electrons must tunnel vertically from Cu-O plane to Cu-O plane through a number of insulating layers before entering into conducting planes which are in intimate electrical contact with the leads out of the sample. A similar argument was required to explain the density-of-states fine structure observed in STM tunneling experiments on Y-Ba-Cu-O.[3] Also, from the known crystal structure of the $TlBa_2(Ca_{0.8}Y_{0.2})Cu_2O_7$, it becomes apparent that the best model for an isolated island with a height of two unit cells is a three-tunnel-capacitor array. The first tunnel capacitor is formed between the tip and surface of the film. The second and third tunnel capacitors must be *identical* and are formed by tunneling between the Cu-O multilayers as shown in Fig. 4.

IV. THREE-TUNNEL-CAPACITOR THEORY

In order to better understand the observed single-electron tunneling structure, a fit was attempted using recent theories[7,8] for multicapacitor arrays such as the one shown schematically in Fig. 5.

In this figure a 1D array of tunnel capacitors is biased by applying a voltage, V, across the entire array. Each tunnel capacitor has a capacitance, an effective resistance, and a particle tunneling rate denoted by C_i, R_i, and Γ_i. An arrow above Γ_i denotes the tunneling direction. For simplicity, the R_i are assumed to be voltage independent.

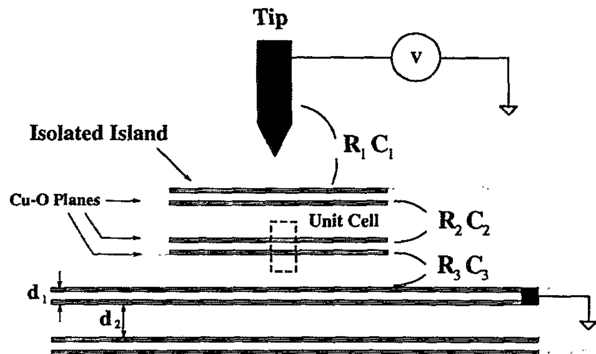

FIG. 4. The layeredlike nature of high-T_c superconductors presents a natural geometry for observing single-electron tunneling by forming ultrasmall capacitances between copper oxide planes on isolated islands. The c-axis unit cell dimension of 1.3 nm and the interplanar spacings d_1 = 0.32 nm and d_2 = 0.96 nm are known from crystallographic studies of the $TlBa_2(Ca_{0.8}Y_{0.2})Cu_2O_7$ material.

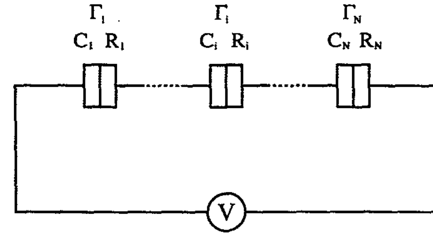

FIG. 5. Schematic of an array of tunnel capacitors connected in series, each capacitor having a tunneling rate, Γ_i, an effective tunnel resistance, R_i, and a capacitance, C_i associated with it. The "Saclay Notation" symbol for an ultrasmall tunnel capacitor capable of single-electron tunneling is used to distinguish the tunnel capacitors from traditional capacitors.

The tunneling rate across a tunnel capacitor can be calculated from a golden-rule assumption to be

$$\mathbf{\Gamma}_i(V, q_1, \ldots, q_{N-1}) = \frac{\mathbf{E}_i(V, q_1, \ldots, q_{N-1})}{e^2 R_i[1 - \exp(\mathbf{E}_i/k_B T)]} , \quad (1)$$

where E_i is the change in energy of the entire system when an electron tunnels across the ith tunnel capacitor in the direction indicated by the arrow. The $E_i(V, q_1, \ldots, q_{N-1})$ are functions of both the bias voltage and the quantized charge on each island in the array. Each q_i represents the charge on the island between the ith and $(i+1)$th tunnel capacitor and thus there are $(N-1)$ such charges. The E_i can be calculated straightforwardly from electrostatic considerations of the change in energy of the array as charges move on and off various islands. Since the expression for E_i is quite complex for a generalized array it is not given here (see Ingold and Nazarov[9] for details).

Tunneling rates in the opposite direction can be calculated by making use of the fact that

$$\mathbf{\Gamma}_i(V, q_1, \ldots, q_{N-1}) = \mathbf{\Gamma}_i(-V, -q_1, \ldots, -q_{N-1}) . \quad (2)$$

If one knows the average charge distribution on each island, $\sigma(V, q_1, \ldots, q_{N-1})$, then the total current through the array is just the net flow through any one tunnel capacitor

$$I(V) = \sum_{q_1, \ldots, q_{N-1}} \sigma(V, q_1, \ldots, q_{N-1}) \times [\mathbf{\Gamma}_i(V, q_1, \ldots, q_{N-1}) - \mathbf{\Gamma}_i(V, q_1, \ldots, q_{N-1})] . \quad (3)$$

In order to use Eq. (3) to calculate $I(V)$, the charge distribution $\sigma(V, q_1, \ldots, q_{N-1})$ must be determined. This is accomplished by making use of the fact that in a steady state, the probability of making a transition between different distributions of charge is zero. This requirement can be expressed as

$$\sigma(V,q_1,\ldots,q_i,\ldots,q_{N-1})[\Gamma_i(q_1,\ldots,q_i,\ldots,q_{N-1})+\Gamma_{i+1}(q_1,\ldots,q_i,\ldots,q_{N-1})]$$
$$=\sigma(V,q_1,\ldots,q_i+e,\ldots,q_{N-1})[\Gamma_i(q_1,\ldots,q_i+e,\ldots,q_{N-1})+\Gamma_{i+1}(q_1,\ldots,q_i+e,\ldots,q_{N-1})]. \quad (4)$$

The distribution $\sigma(V,q_1,\ldots,q_{N-1})$ can be calculated by using an arbitrary assumption for any particular distribution of charges and iteratively calculating the relative probability for all of the other charge distributions using Eq. (4). The final result can then be normalized using the requirement that for each voltage

$$\sum_{q_1,\ldots,q_{N-1}} \sigma(V,q_1,\ldots,q_{N-1})=1. \quad (5)$$

Equations (2)–(5) cannot be solved analytically without making considerable simplifications which result in the loss of many important details. In addition, a fractional charge Q_i may exist on each island, permitting the entire curve to be shifted left or right of the origin. These Q_i also add some asymmetry to the detailed shape of the $I(V)$ curve.

Based on these equations, we have developed a computer program which can calculate a best fit to $I(V)$ data for three-capacitor arrays ($N = 3$) by searching over a wide range of parameter space. A best fit amounts to finding a global minima in the root-mean-square deviation of a theoretical calculation from experimental data while allowing the C_i, R_i, Q_i, and possibly T to vary. Since neither $I(T,V;C_1,\ldots,C_N,R_1,\ldots,R_N,Q_1,\ldots,Q_{N-1})$ nor its partial derivatives can be represented analytically, finding a global best fit is computationally intensive. Traditional techniques such as the "method of steepest descent" are of limited use since numerically calculating the partial derivatives is time consumptive. Alternatively, a search over a wide range of parameters at a coarse resolution and then narrowing in on the best prospects can lead to a local rather than global best fit. Our approach was to use the Coulomb gap around $V = 0$ along with the overall slope of the $I(V)$ data to put some limits on the range of values over which our variables could vary. Then, a thorough search for a best fit within this realistic range was performed.

V. COMPARISON OF THREE-TUNNEL-CAPACITOR THEORY TO STM TUNNEL DATA

Much of the spectroscopic data obtained during the course of this study exhibited linear $I(V)$ curves with only a slight overall curvature. Since no evidence for a superconducting gap was observed, it can be concluded that the surface was normal even though the bulk of the sample was observed to be superconducting by magnetization measurements.[1] This lack of a superconducting gap is frequently observed in high-T_c materials and is often attributed to surface degradation. Surface degradation can be caused by outdiffusion of oxygen, a nonstoichiometric surface layer,[10] or the formation of a contamination layer at the surface.[11]

In contrast to this behavior, some regions on the sample revealed nonlinear $I(V)$ behavior clearly related to single-electron behavior. A typical measurement of this structure is shown in Fig. 6. This data was taken at 9.8 K and was quite reproducible over a period of hours. Similar structure was observed at other locations on the film. The data are from a single sweep of the voltage between the STM tip and film and are unfiltered in any way.

Figure 6 also shows a best fit to the data using a three-tunnel-capacitor model as described in Sec. IV. A stringent requirement in this fitting procedure is that the interlayer capacitances and resistances for two of the tunnel capacitors must be identical. *A priori*, it was not clear whether this restriction would allow a reasonable fit to the data. Since the curve was nearly symmetric about $V = 0$, no fractional charges were required. The fitting procedure required four independent variables, with the best values of $C_3 = C_2 = 3.3\times10^{-18}$ F, $C_1 = 2.2\times10^{-19}$ F, $R_3 = R_2 = 1.7\times10^{7}\ \Omega$, and $R_1 = 9.0\times10^{6}\ \Omega$. A two-tunnel-capacitor fit using four parameters yielded a poorer fit.[1] A comparison of these fits is shown in Table I. The bottom line of this table shows the root-mean-square (rms) deviation per point for the best fits using the two models. Although the two-tunnel-capacitor model provides a reasonable fit, the rms is 25% higher than the three-tunnel-capacitor model, with both models having

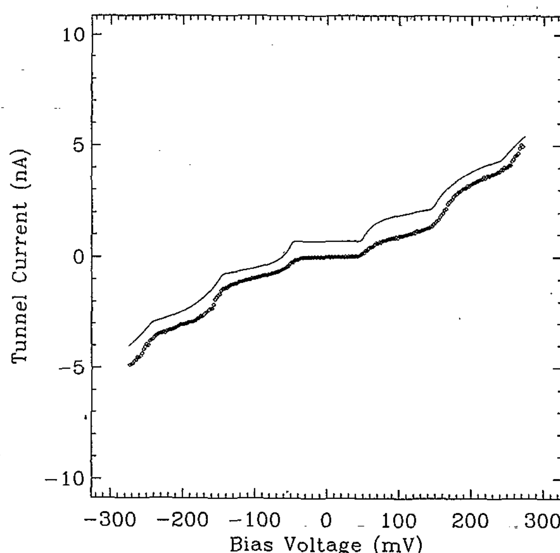

FIG. 6. A fit (solid line) to the tunneling data (diamonds) using the three-tunnel-capacitor model described in the text. The theoretical fit for the three-tunnel-capacitor model is shifted vertically for the purposes of clarity, and was obtained using values of $C_1 = C_2 = 3.3\times10^{-18}$ F, $C_3 = 2.2\times10^{-19}$ F, $R_1 = R_2 = 1.7\times10^{7}\ \Omega$, and $R_3 = 9.0\times10^{6}\ \Omega$.

TABLE I. A comparison of the two- and three-junction fits to the data. Note that since the three-junction fit was confined such that $R_2 = R_3$ and $C_2 = C_3$ both methods had four independent fitting parameters. The far right column shows estimates of values for resistances and capacitances consistent with the proposed geometry.

	2-Jct. Model	3-Jct. model	Estimated values
R_1 (Ω)	4.3×10^6	9.0×10^6	$10^6 - 10^{10}$
R_2 (Ω)	3.9×10^7	1.7×10^7	$10^6 - 10^7$
R_3 (Ω)	–	1.7×10^7	$10^6 - 10^7$
C_1 (F)	1.0×10^{-19}	2.2×10^{-19}	$10^{-19} - 10^{-20}$
C_2 (F)	1.6×10^{-18}	3.3×10^{-18}	$10^{-17} - 10^{-18}$
C_3 (F)	–	3.3×10^{-18}	$10^{-17} - 10^{-18}$
rms (nA)	0.20	0.16	–

the same number of fitting parameters. We were able to obtain these fits without using an αV^3 that has frequently been used in published results for two-capacitor fits.[12] Often both a cubic term and a fractional charge are used in two-capacitor fits, resulting in six independent fitting variables. Our attempts at using these additional parameters resulted in only moderately better fits at the expense of additional fitting parameters.

The improvement in the fit over that reported previously[1] is best observed statistically by some "goodness of fit" criterion such as the rms values discussed previously, however, comparing the derivative of the of the data to the calculated conductance as shown in Fig. 7 is also instructive. In this figure we display the derivative of the best three-capacitor fit to the experimental data. For completeness, we also show the best two-tunnel-capacitor fit.[1] This comparison reveals some interesting trends not readily apparent from the overall fit to the $I(V)$ data displayed in Fig. 6.

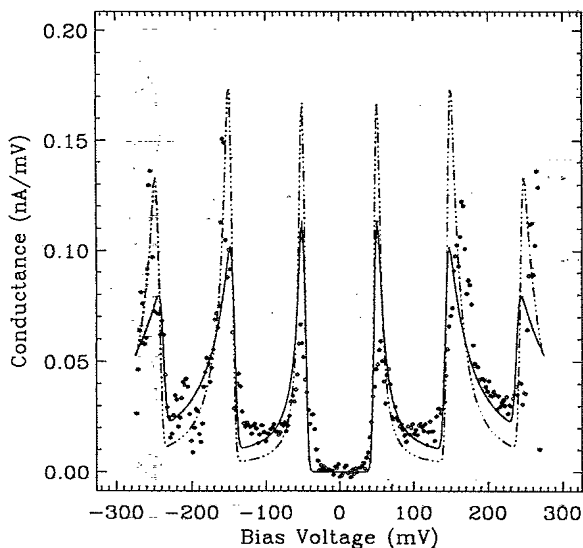

FIG. 7. A fit (solid line) using the three-tunnel-capacitor model to the derivative of the tunneling data (diamonds) is displayed. For purposes of comparison, the best two-tunnel-capacitor fit (dashed line; Ref. 1) is also shown.

First, the addition of a third tunnel capacitor substantially decreases the conductance at the first step located near ±55 mV. The decrease in conductance over that found for the two-capacitor fit is not sufficient to match the value found experimentally, but a significant improvement is evident. However, as the tunneling voltage increases, the value of the conductance at the second step is in better agreement with the three-tunnel-capacitor model. At still higher bias voltages, the data are best fit by the two-capacitor model. This trend suggests that a four-capacitor model would provide a better fit to the data at low bias voltage. It also follows that the number of tunnel capacitors required to fit the data might decrease as the bias voltage increases. This observation provides a suggestion that the applied bias voltage may influence the tunneling rate between the various conducting layers.

Apart from the improved fit to the conductance at each step, the three-capacitor model reproduces the data much better in the plateau regions of Fig. 6. This is apparent in Fig. 7 by inspecting the fit to the local minima in the conductance data. Finally, a slight asymmetry in the location of the steps for positive and negative bias voltages is evident from the conductance data plotted in Fig. 7. The asymmetry is beyond that expected from our digital control electronics and may be related to an inherent asymmetry between hole (tip positive) and electron (tip negative) tunneling into this thin film material.

We also attempted to further improve the fit by increasing the temperature above 10 K, since recent work has suggested that nonequilibrium effects may be important in small tunnel structures.[13] However, for the case under study here, no significant improvement in the overall fit was obtained.

VI. DISCUSSION

In an STM experiment, one tunnel capacitor can always be attributed to the tip-sample spacing. In order to fully understand single-electron tunneling data, it is important to identify the origin of all the tunnel capacitors, since one capacitor alone is insufficient to produce a complicated $I(V)$ structure. For the case under consideration here, we have suggested that the tunnel capacitor can be naturally attributed to the interlayer capacitance of isolated islands which occur in this planar high-T_c material. It is useful to estimate the value of the interlayer capacitances and resistances expected and to compare these estimates to those obtained from the model.

The unit cell of $TlBa_2(Ca_{0.8}Y_{0.2})Cu_2O_7$ is tetragonal with $a = 0.39$ nm, and $c = 1.3$ nm.[14] An important feature of the cell is that it consists of pairs of conducting (or superconducting) Cu-O sheets. Each Cu-O sheet is 0.32 nm from its nearest-neighboring Cu-O plane with a single Ca-O layer in between. The paired Cu-O planes are 0.96 nm from the next-nearest paired Cu-O plane, with two Ba-O layers and a Tl-O layer in between. All of the planes are perpendicular to the c axis and thus are parallel to the surface. The existence of these Cu-O planes separated by insulatinglike material leads to the

possibility of ultrasmall tunnel capacitors being formed between them.

Topographic scans of this material (and other layered-like high-T_c materials) frequently exhibit a stacked-disk growth mode. This growth mode often leads to disconnected islands on the uppermost layer. These islands present a likely structure for the formation of an ultrasmall parallel plate capacitor. To calculate the capacitance such a geometry might produce, we consider one of the disconnected islands in Fig. 1 as a parallel plate capacitor system illustrated in Fig. 4. Using $C = \kappa\epsilon_0 A/d$ one can estimate whether or not this presents a viable mechanism.

From topographical data such as in Fig. 1, islands with areas of $A = 1 - 100$ nm^2 and heights of two unit cells are clearly present. Typically, $A = 25$ nm^2. Nearest-neighbor planes (with a spacing of $d_1 = 0.3$ nm) are so close that for practical purposes they can be considered a single plane. Assuming a dielectric constant of $\kappa \sim 5$ and the known next-nearest-neighbor spacing between planes of $d_2 = 1$ nm leads to capacitances of $\sim 10^{-18}$ F. Although it is difficult to estimate the appropriate dielectric constant to use for the interplanar Tl-O and Ba-O material, the calculation is not very sensitive to this parameter. Such a calculation is clearly only order of magnitude, but it demonstrates that the interplanar capacitance of these layered materials is consistent with the parameters $C_3 = C_2 = 3.3 \times 10^{-18}$ F required to fit the data in Fig. 6. The tip-to-sample capacitance, C_1, can be crudely estimated from modeling the tip as a small sphere of diameter d and calculating the self capacitance of the sphere next to an infinite conducting plane, where $C = 2\pi\epsilon_0 d$. Using values of $d \sim 10^{-8} - 10^{-9}$ m leads to an expected C_1 of $10^{-19} - 10^{-20}$ which is consistent with the fitting values used in Table I.

The resistance between two paired Cu-O planes can also be roughly estimated. First, the validity of viewing c-axis conduction as tunneling between the paired Cu-O planes is supported by the observation that the c-axis resistivity increases exponentially with the adjacent Cu-O multilayer distance in these materials.[14] The resistance to current flow through an island can be estimated in two different ways. The c-axis resistivity in $TlBa_2(Ca_{0.8}Y_{0.2})Cu_2O_7$ is not known, but the c-axis resistivity in the parent compound $TlBa_2CaCu_2O_7$ is quite high with a value of $\rho = 2$ Ω cm being typical.[14] Using this value, an order of magnitude estimate of the resistance between the paired Cu-O planes can be made. Assuming uniform current flow, $R = \rho l/A$, where $l \sim d_2 = 1$ nm, $A = 25$ nm^2, and $\rho = 2$ Ω cm. This gives a lower limit resistance of approximately 10^6 Ω. Realizing that a current injection process is more likely to characterize the current flow through an island provides a better way to estimate the resistance. It is well known[15] that the spreading resistance for current flow into a flat plane of resistivity ρ through a small spot of radius a is given by $R = \rho/4a$. For current injection from an STM tip, $a \sim 0.3$ nm, giving a value for $R = 1.7 \times 10^7$ Ω. This latter estimate is in particularly good agreement with the parameter $R_3 = R_2 = 1.7 \times 10^7$ Ω required to fit the data. The tip-to-sample tunnel resistance, R_1, is difficult to independently verify but values from 10^6 to 10^{10} are quite possible using typical tip-to-sample spacings and cross sectional tunneling areas.

Finally, it is worth pointing out that layered materials of the type studied here make an attractive material for fabricating 1D arrays of tunnel capacitors. By vertically etching away material from a flat layered surface one can visualize the fabrication of stacked arrays of ultrasmall capacitors connected in a series configuration. In this regard it is instructive to note that for an array of N equal tunnel capacitors with capacitance C, the spacing between steps as well as the zero-bias Coulomb gap is given by $\pm(N-1)(e/2C)$.[9]

It follows that the width of the steps in the Coulomb staircase can be adjusted by controlling the number of capacitors in an array. The opportunity to achieve this using the natural layered structure of materials like $TlBa_2(Ca_{0.8}Y_{0.2})Cu_2O_7$ is appealing. It should be noted in this context that if one capacitor is significantly larger than the others, it will have a dominating effect.

A 1D array of tunnel capacitors fabricated from a layered material also is advantageous for producing practical circuit elements based on single-electron tunneling effects, where replacing single-tunnel-capacitor elements by larger 1D arrays can dramatically improve cir-

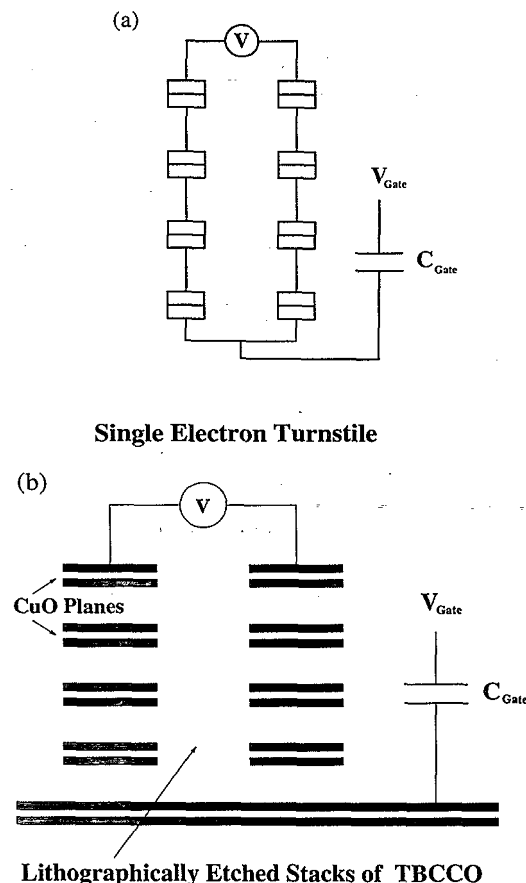

FIG. 8. A capacitively coupled single-electron turnstile. In (a), a typical single-electron turnstile circuit as discussed in Ref. 17. In (b), an equivalent circuit that could be fabricated from a suitable layered material such as the high-T_c compound discussed here.

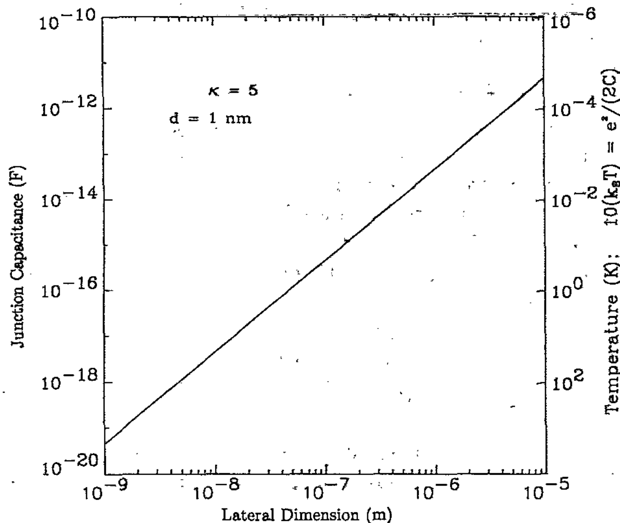

FIG. 9. A plot of tunnel capacitance vs lateral dimension for a single-electron device fabricated from a multilayer thin film with interplanar spacing $d = 1$ nm and $\kappa = 5$. The right abcissa provides an estimate for the operating temperature of such a device as a function of lateral dimension and serves as a rough guide for the lateral resolution required by a nanolithographic process to produce a working device at a specified temperature.

cuit performance.[16] This point is made more clearly in Fig. 8(a) which illustrates a schematic of a single-electron turnstile circuit. This circuit is a three-terminal device that allows a single electron to be passed through two electrodes when a voltage pulse is applied to the third electrode. A possible implementation produced by etching out stacks of tunnel capacitors from a layered material is shown in Fig. 8(b). This is only one example selected from a wide class of useful electronic devices[17] that can be fabricated from stacked tunnel-capacitor arrays described above.

Considerable improvement can be anticipated if the starting film for such fabrication consists of molecular beam epitaxy (MBE) high-T_c material like $Bi_2Sr_2CaCuO_8$ film.[18] The low defect density coupled with the ability to control the interplanar spacing using standard MBE growth techniques permits considerable versatility in tailoring the intraplanar capacitance and tunneling resistance. Steady progress in the lithographic patterning of high-T_c films has been reported,[19–21] resulting in features as small as 2–3 μm.[20] Using ion milling, features as small as 1 μm have also been produced.[22,23]

These capabilities suggest that remarkable improvements in the operating temperature for single-electron devices can be expected when arrays of tunneling capacitors are fabricated from layered films. Figure 9 illustrates this by plotting tunnel capacitor size vs tunnel capacitance for typical values of $\kappa = 5$ and $d = 1$ nm. Also plotted on the right vertical axis is an equivalent temperature, defined as $\gamma k_b T = e^2/(2C)$ (eV), at which the operation of such a device will become practical. Although an exact value for γ depends upon the application in question, for the purposes of this plot we set $\gamma = 10$, a value consistent with discussions found in the literature.[16,24]

VII. CONCLUSIONS

A previous suggestion[1] that the layeredlike nature of high-T_c materials results in the formation of ultrasmall capacitances which lead to single-electron charging effects has been further investigated. Spectroscopic $I(V)$ data obtained on a $TlBa_2(Ca_{0.8}Y_{0.2})Cu_2O_7$ film are reanalyzed using a more realistic three-tunnel-capacitor model. When compared to a fit based on a two-tunnel-capacitor model, considerable improvement in the overall fit to the measured conductance is found. It is likely that single-electron charging effects are not unique to the $TlBa_2(Ca_{0.8}Y_{0.2})Cu_2O_7$ material and that similar effects may occur in a much larger class of layered materials. The utility of using a layered thin film to fabricate nanoelectronic devices operating on single-electron principles has also been emphasized.

ACKNOWLEDGMENTS

The authors would like to thank K. Likharev for helpful comments during the early stages of this work. This work was supported in part by ARO Contract No. DAAL03-92-G-0144 and DOE Contract No. DE-FG02-90ER45427.

[1] T.G. Miller, R. Reifenberger, M.W. McElfresh, D.W. Face, and W.L. Holstein, J. Low Temp. Phys. **94**, 239 (1994).
[2] D.W. Face and J.P. Nestlerode, Appl. Phys. Lett. **61**, 1838 (1992).
[3] T.G. Miller, M.W. McElfresh, and R. Reifenberger, Phys. Rev. B **48**, 7499 (1993).
[4] J.W. Lyding, S. Skala, J.S. Hubacek, R. Brockenbrough, and G. Gammie, Rev. Sci. Instrum. **59**, 1897 (1988).
[5] Ch. Renner, Ph. Niedermann, A.D. Kent, and O. Fischer, J. Vac. Sci. Technol. A **8**, 330 (1990).
[6] Ch. Renner, Ph. Niedermann, A.D. Kent, and O. Fischer, Rev. Sci. Instrum. **61**, 965 (1990).
[7] M. Amman, R. Wilkins, E. Ben-Jacob, P.D. Maker, and R.C. Jaklevic, Phys. Rev. B **43**, 1146 (1991).
[8] A.E. Hanna and M. Tinkham, Phys. Rev. B **44**, 5919 (1991).
[9] *Single Charge Tunneling: Coulomb Blockade Phenomena in Nanostructures*, edited by H. Grabert and M.H. Devoret (Plenum, New York and London, 1992).
[10] A.J. Drehman, M.W. Dumais, and J.A. Horrigan, J. Mater. Res. **5**, 1392 (1990).
[11] T.G. Miller, M.W. McElfresh, and R. Reifenberger, Phys. Rev. B **48**, 7499 (1993).
[12] R. Wilkins, M. Amman, R.E. Soltis, E. Ben-Jacob, and

R.C. Jaklevic, Phys. Rev. B **41**, 8904 (1990).
[13] N. Garcia and F. Guinea, Phys. Rev. B **46**, 571 (1992).
[14] D.H. Kim, K.E. Gray, R.T. Kampwirth, J.C. Smith, D.S. Richeson, T.J. Marks, J.H. Kang, J. Talvacchio, and M. Eddy, Physica C **177**, 431 (1991).
[15] R.G. Mazur and D.H. Dickey, J. Electrochem. Soc. **113**, 255 (1966).
[16] K.K. Likharev, IEEE Trans. Magn. **23**, 1142 (1987).
[17] D.V. Averin and K.K. Likharev, in *Single Charge Tunneling*, edited by H. Grabert and M.H. Devoret (Plenum, New York, 1992), pp. 311–331.
[18] D.G. Schlom, A.F. Marshall, J.T. Sizemore, Z.J. Chen, J.N. Eckstein, I. Bozovic, K.E. Von Dessonneck, J.S. Harris, Jr., and J.C. Bravman, J. Cryst. Growth **102**, 361 (1990).
[19] P. Cocciolo, M. Gentili, C. Giovannella, M. Iannuzzi, L. Luciani, V. Merlo, R. Messi, and L. Paoluzi, J. Less-Common Met. **164-5**, 374 (1990).
[20] J.J. Kingston, F.C. Wellstood, D. Quan, and J. Clarke, IEEE Trans. Magn. **27**, 974 (1991).
[21] M. Danerud, M.E. Gershenson, Z. Ivanov, D. Winkler, and T. Claeson, Physica C **185-189**, 1939 (1991).
[22] A. Enokihara, H. Higashino, K. Setsune, T. Mitsuyu, and K. Wasa, Jpn. J. Appl. Phys. Lett. **27**, L1521 (1988).
[23] Z.G. Ivanov, P-A. Nilsson, E-K. Andersson, and T. Claeson, Supercond. Sci. Technol. **4**, 112 (1991).
[24] D.V. Averin and K.K. Likharev, J. Low Temp. Phys. **62**, 345 (1986).